*Journal of*
*Nanoscience and Nanotechnology*
Vol. 12, 8029–8033, 2012

# Single-Crystalline $Bi_2S_3$ Nanobelts: Hydrothermal Synthesis and Growth Mechanism

Ruimin Xing[1], Deliang Li[1], Caixia An[2], Ling Zhang[1], Qiaoling Li[1], and Shanhu Liu[1,*]

[1] *Institute of Molecular and Crystal Engineering, College of Chemistry and Chemical Engineering, Henan University, Kaifeng, Henan 475004, P. R. China*
[2] *School of Chemistry and Chemical Engineering, Henan Institute of Science and Technology, Xinxiang 453003, P. R. China*

High-quality single-crystalline $Bi_2S_3$ nanobelts were synthesized with $Bi(NO_3)_3 \cdot 5H_2O$ and thioacetamide (TAA) as the raw materials in the polyvinylpyrrolidone (PVP) aqueous solution via a facile hydrothermal route. The morphology and crystallinity of the nanobelts were characterized by X-ray powder diffraction (XRD), field emission scanning electron microscopy (FESEM), X-ray energy dispersive spectroscopy (EDX), transmission electron microscopy (TEM), and selected area electron diffraction (SAED). The effects of a series of reaction parameters on the morphology of $Bi_2S_3$ were studied. A plausible growth mechanism based on preferred orientation growth is proposed to address the formation of $Bi_2S_3$ nanobelts.

**Keywords:** Nanostructure, Hydrothermal, Nanobelts, Bismuth Sulfide.

RESEARCH ARTICLE

## 1. INTRODUCTION

One-dimensional (1D) semiconductor nanomaterials have extensively been studied because they serve as model materials for understanding fundamental physical phenomena and also for constructing nanoscale devices with improved performance.[1–9] Various strategies, including electrospining, template method, thermal oxidation, and biomimetic synthesis, have been developed for the preparation of different kinds of 1D semiconductor nanostructures.[10–20] Among all these semiconductors, chalcogenide semiconductor 1D nanostructures have attracted broad attention because of their unique shape- and size-dependent physical and chemical properties that differ drastically from their bulk counterparts.[21–27] As an important chalcogenide semiconductor with a direct band gap of 1.3 eV, bismuth sulfide ($Bi_2S_3$) has attracted particular interest in practical applications as photodiode arrays, photovoltaic converters, and thermoelectric cooling technologies based on the Peltier effect.[28–30] Although great effort has been directed in the synthesis of 1D $Bi_2S_3$ nanostructures, such as nanorods, nanowires, nanoribbons, and nanotubes,[31–34] fabrication of high-quality 1D $Bi_2S_3$ nanostructures in aqueous solution is still a challenge. In particular, current synthetic routes for $Bi_2S_3$ nanobelts were mostly involved in organic solvents or mixed solvents.[35–37] In this paper, high quality single-crystalline $Bi_2S_3$ nanobelts were prepared by using $Bi(NO_3)_3 \cdot 5H_2O$ and thioacetamide (TAA) as the raw materials in the PVP aqueous solution via a facile hydrothermal procedure. Effects of a series of reaction parameters on the morphology of $Bi_2S_3$ nanostructures were studied. In addition, a plausible growth mechanism of $Bi_2S_3$ nanobelts was also discussed.

## 2. MATERIALS AND METHODS

### 2.1. Materials

Poly(vinylpyrrolidone) (PVP, K30, $M_w = 40{,}000$) was purchased from Sigma-Aldrich Chemical Reagent Co., Ltd. $Bi(NO_3)_3 \cdot 5H_2O$, TAA and other chemical reagents were of analytical grade and used as received without further purification. Millipore water (18.2 MΩ cm at 25 °C) was used throughout all experiments.

### 2.2. Methods

#### *2.2.1. Preparation of $Bi_2S_3$ Nanobelts*

In a typical process, 5 mL of 30 mmol $L^{-1}$ $Bi(NO_3)_3$ aqueous solution and 10 mL of 5 mg $mL^{-1}$ of PVP mixed with vigorous stirring and a white suspension was formed and stirred for 3 h. After adding 5 ml of 90 mmol $L^{-1}$ TAA aqueous solution, the suspension slowly changed to black,

*Author to whom correspondence should be addressed.

indicating the formation of colloidal $Bi_2S_3$ nuclei. After overnight aging, the suspension was sealed in autoclaves (volume of autoclaves is 25 mL), and subsequently heated to 200 °C for 12 hours. The products were collected and washed at least three times with water and ethanol, then dried under vacuum before characterization.

In control experiments, the effects of a series of reaction parameters on the morphology of $Bi_2S_3$ were studied. In Control *A* experiment, the $Bi(NO_3)_3$ aqueous solution mixed with the PVP aqueous solution, which was adjusted to pH 1 to avoid the hydrolyzation of $Bi^{3+}$ into $BiONO_3$. To investigate the influence of the concentrations on the morphology of the products, the other two sets of the control experiments were carried out. Control *B* was to vary the initial concentration of $Bi(NO_3)_3$ and TAA in the reaction. Control *C* was to vary the concentration of PVP. The rest of the synthesis conditions in each of control experiments were kept the same as in the typical experiment described above.

#### *2.2.2. Characterization*

FE-SEM images and EDX spectra were obtained using Hitachi S-4800 Field Emission Electron Microscope at an accelerating voltage of 10 kV. TEM images and SAED patterns were taken using a JEOL JEM-2100 Transmission Electron Microscope at an accelerating voltage of 200 kV. XRD measurements were performed on a Japan Shimadzu XRD-6000 Diffractometer with Cu K$\alpha$ radiation; a scanning rate of 0.05 deg/s was applied to record the patterns in the $2\theta$ range of 10°–80°.

## 3. RESULTS AND DISCUSSION

### 3.1. Characterization of as-Prepared $Bi_2S_3$ Nanobelts

The crystal structures were studied by XRD analyses. As shown in Figure 1, the strong and sharp diffraction peaks in the pattern show that the as-obtained product was well crystallized. All the diffraction peaks and positions can be indexed to orthorhombic phase of $Bi_2S_3$ (cell constants: $a = 11.150$ Å, $b = 11.300$ Å, $c = 3.9817$ Å, JCPDS card No. 43-1471).

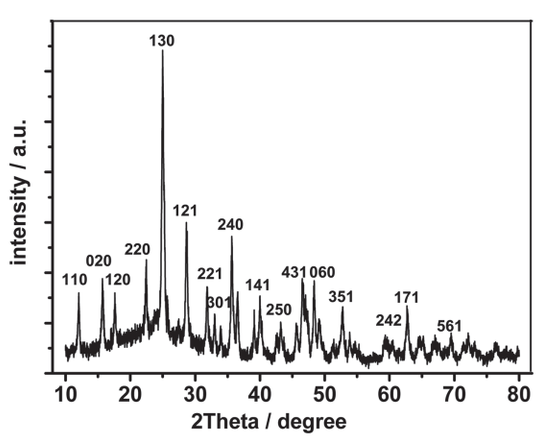


**Fig. 1.** XRD pattern of $Bi_2S_3$ nanobelts obtained in the typical experiment.

The morphology and size of the products were investigated by SEM and TEM analyses. Figure 2(a) reveals that the product presents the belt-like structure and the nanobelts have the sizes of a few micrometers in length and tens of nanometers in width. The corresponding EDX spectra in Figure 2(b) show the significant presence of Bi and S, besides the peaks for Cu and C arise from the copper base used in the sample preparation. Based on the relative area under the peaks, the atomic ratio of Bi and S is evaluated to be approx. 2:3, in good agreement with the stoichiometric molar ratio of $Bi_2S_3$. The TEM image in Figure 2(c) confirms the belt-like geometry of $Bi_2S_3$ nanostructures. Its SAED pattern recorded on an individual nanobelt reveals the single crystalline nature of the material (inset of Fig. 2(c)). More evidence on its structure and crystallinity was obtained from high-resolution TEM image (HRTEM) (Fig. 2(d)). The interplanar *d* spacings are 0.56 nm, corresponding to the (200) lattice planes of $Bi_2S_3$. The corresponding Fast Fourier Transform (FFT) pattern (inset of Fig. 2(d)) indicates that the nanobelts are single crystallines with the [100] growth direction.

### 3.2. Possible Formation Mechanism of $Bi_2S_3$ Nanobelts

To investigate the growth process of these nanobelts, several sets of control experiments were performed and the products were studied by using SEM, as discussed below. In a typical experiment, $Bi(NO_3)_3$ firstly hydrolyzed in the PVP aqueous solution to produce a white suspension of $BiONO_3$. Once $S^{2-}$ ions were introduced and released from TAA solution, the suspension slowly changed to black, indicating the formation of $Bi_2S_3$ nuclei at the expense of $BiONO_3$. The reason is that the solubility constant of $Bi_2S_3$ ($1 * 10^{-97}$) is extraordinarily smaller than that of $BiONO_3$ ($2.82 * 10^{-3}$).[38] The product obtained after overnight aging and without hydrothermal treatment are mainly nanospheres with a lot of short rod-like nanowhiskers on the surface (Fig. 3(a)). In Control *A* experiment, otherwise, the $Bi(NO_3)_3$ aqueous solution was mixed with the PVP aqueous solution and adjusted to pH 1, in which the clear solution presented and no white precipitate appeared, suggesting $Bi^{3+}$ ions instead of $BiONO_3$ exist in the reaction solution. Here, $Bi^{3+}$ ions may coordinate with some groups of PVP. After the addition of TAA, the clear solution slowly changed to black, indicating the formation of $Bi_2S_3$ nuclei. In spite of the same following hydrothermal treatment, the nanobelts were obtained in the typical experiment while the stout rod-like products appeared in Control *A*. When without hydrothermal treatment in another control experiment,

RESEARCH ARTICLE

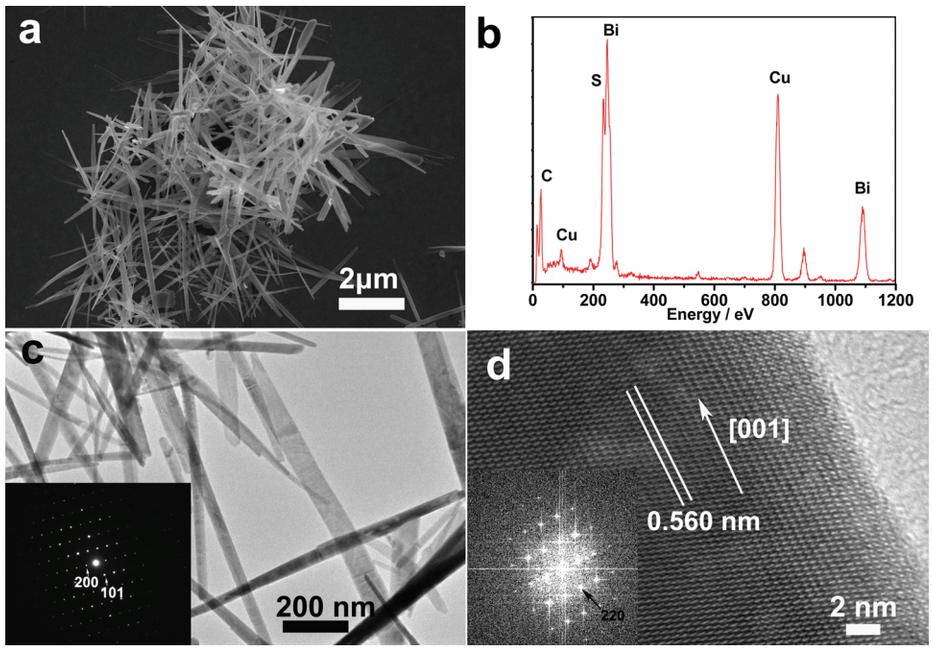


**Fig. 2.** (a) SEM image; (b) EDX spectra; (c) low-resolution TEM (inset is the SAED patterns); and (d) HRTEM images (inset is the corelative FFT patterns) of the $Bi_2S_3$ nanobelts obtained in the typical experiment.

there are not belt-like nanostructures but some urchin-like and sphere-like nanostructures in appearance (Fig. 3(b)). In the absence of PVP, only irregular bulk particles were formed (Fig. 3(c)). These results indicate that the intermediate product of $BiONO_3$ and the hydrothermal treatment as well as PVP are crucial in the formation of the nanobelts.

On the other hand, the concentrations of reagents usually play an important role in the formation of the nanostructures.[39–41] In Control *B* experiment, when the concentration of $Bi(NO_3)_3$ was decreased to 5 mmol $L^{-1}$, as shown in the Figure 4(a), the nanowires were obtained with the sizes of several micrometers in length and *ca.* 50 nm in diameter. When the concentration of $Bi(NO_3)_3$ was increased to 50 mmol $L^{-1}$, as shown in the Figure 4(b), the nanosheets appeared with shorter lengths and lower aspect ratios compared to the nanobelts; they are assembled to be a hierarchical nanostructure, just like a bunch of firecracker. Further increasing the concentration of $Bi(NO_3)_3$ up to 100 mmol $L^{-1}$ results in the irregular morphology, in which nanobelts, nanosheets and nanorods coexist (Fig. 4(c)). The results suggest the more the initial concentration of $Bi(NO_3)_3$, the lower aspect ratio the product exhibit with an increase in morphological diversity. On the other hand, with increasing the concentration of PVP from 1 mg $mL^{-1}$ to 10 mg $mL^{-1}$, the products exhibit 1D nanotructures with a decrease in the aspect ratio. The results indicate that PVP is beneficial to the formation of nanobelts or other 1D nanostructures in this reaction system.

On the basis of the above observations and discussion, a plausible mechanism based on preferred orientation growth is proposed to address the formation of $Bi_2S_3$ nanobelts. The process might be involved in two stages: nucleation at low temperature and subsequent growth at high temperature. $Bi(NO_3)_3$ firstly hydrolyzed in the PVP aqueous solution to produce $BiONO_3$. Once $S^{2-}$ ions were introduced, $Bi_2S_3$ nuclei come into being at the expense of $BiONO_3$. In the second stage, the higher temperature and pressure as well as PVP are important for the nucleis growth.

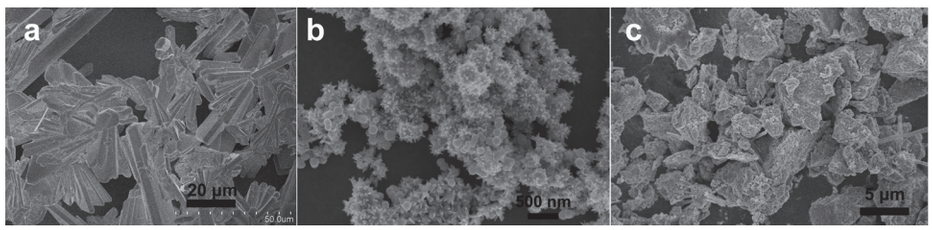


**Fig. 3.** SEM images of the $Bi_2S_3$ nanostructures prepared at different conditions. (a) The pH of the mixed solution was adjusted to 1 with 6 M $HNO_3$, (b) without hydrothermal treatment, and (c) without PVP.

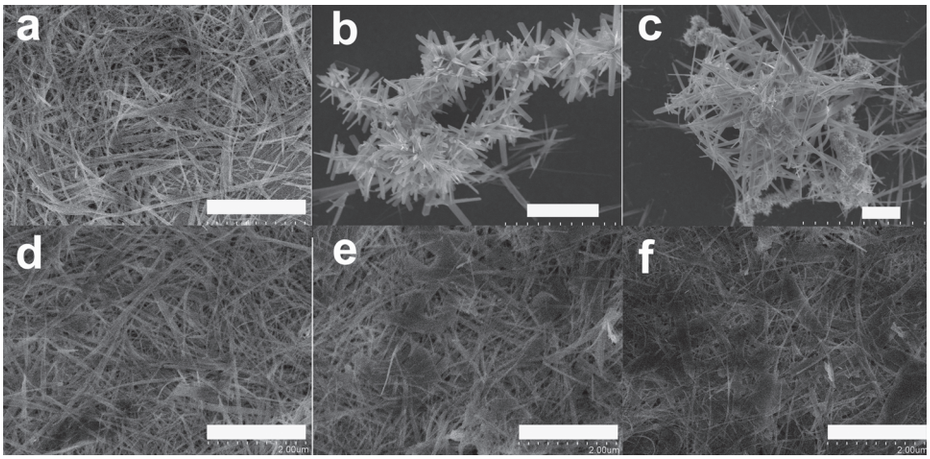


**Fig. 4.** SEM images of the $Bi_2S_3$ prepared at different concentration of reagents. (a) 5 mmol $L^{-1}$ $Bi(NO_3)_3$, (b) 50 mmol $L^{-1}$ $Bi(NO_3)_3$, and (c) 100 mmol $L^{-1}$ $Bi(NO_3)_3$. (The corresponding concentration of TAA was 15, 150, and 300 mmol $L^{-1}$, respectively, with keeping the same stoichiometric molar ratio of Bi to S); (d) 1 mg $mL^{-1}$ PVP, (e) 3 mg $mL^{-1}$ PVP, and (f) 10 mg $mL^{-1}$ PVP. All the scale bar are 2 $\mu$m.

The orthorhombic $Bi_2S_3$ has a highly anisotropic layered structure. It consists of infinite ribbon-like $Bi_4S_6$ polymers, which are linked together by inter-molecular attraction between Bi and S atoms.[29] The chain-like building blocks are parallel to the c-axis. Therefore, the orthorhombic phase $Bi_2S_3$ has a tendency toward 1D growth along the [100] direction, which then led to the formation of 1D nanostructures. Under the hydrothermal process and also with the help of PVP, the relative high nucleis concentration will grow into the belt-like structures driven by the anisotropic growth tendency of $Bi_2S_3$.

## 4. CONCLUSIONS

In summary, high-quality single-crystalline $Bi_2S_3$ nanobelts were synthesized with $Bi(NO_3)_3 \cdot 5H_2O$ and thioacetamide (TAA) as the raw materials in the PVP aqueous solution via a facile hydrothermal procedure. The effect of a series of reaction parameters on the morphology of $Bi_2S_3$ were studied. A plausible growth mechanism based on preferred orientation growth is proposed to address the formation of $Bi_2S_3$ nanobelts. The aqueous solution synthetic route is cost-effective and easy to maintain and control without using organic solvent, which may be used in the preparation of other 1D nanostructures.

**Acknowledgments:** This work was financially supported by National Natural Science Foundation of China (21101056, 21105021) and Educational Commission of Henan Province of China (2011A150005).

## References and Notes

1. T. H. Ji, L. Y. Dong, Y. Liu, L. Li, and B. G. Sun, *J. Nanosci. Nanotechnol.* 11, 3861 (**2011**).
2. L. A. Li, P. C. Wu, X. S. Fang, T. Y. Zhai, L. Dai, M. Y. Liao, Y. Koide, H. Q. Wang, Y. Bando, and D. Golberg, *Adv. Mater.* 22, 3161 (**2010**).
3. S. K. Batabyal, C. Basu, A. R. Das, and G. S. Sanyal, *J. Nanosci. Nanotechnol.* 7, 565 (**2007**).
4. I. Jung, Y. Kwon, J. Lee, and B. Min, *J. Nanosci. Nanotechnol.* 11, 6555 (**2011**).
5. R. M. Xing, S. H. Liu, and S. Tian, *J. Nanopart. Res.* 13, 4847 (**2011**).
6. Y. R. Tao, Q. X. Gao, X. F. Wang, X. C. Wu, C. J. Mao, and J. J. Zhu, *J. Nanosci. Nanotechnol.* 11, 3345 (**2011**).
7. Y. Q. Chen, Y. Shao, X. H. Zhang, C. Jia, Y. Su, Q. Li, L. Z. Liu, and T. B. Guo, *J. Nanosci. Nanotechnol.* 11, 1205 (**2011**).
8. W. Kubo, H. Hayakawa, K. Miyoshi, and S. Fujikawa, *J. Nanosci. Nanotechnol.* 11, 131 (**2011**).
9. L. Miao, S. Tanemura, R. Huang, C. Y. Liu, C. M. Huang, and G. Xu, *J. Nanosci. Nanotechnol.* 11, 9267 (**2011**).
10. Y. L. Cheng, W. Z. Huang, Y. F. Zhang, L. Zhu, Y. J. Liu, X. Z. Fan, and X. Q. Cao, *Cryst. Eng. Comm.* 12, 2256 (**2010**).
11. N. Hoa, H. Heo, J. Lim, G. Kim, and E. Kim, *J. Nanosci. Nanotechnol.* 12, 1411 (**2012**).
12. G. D. Wei, G. Zhang, F. Gao, J. Zheng, Y. Qin, W. Han, W. Qin, and W. Yang, *J. Nanosci. Nanotechnol.* 11, 9752 (**2011**).
13. Y. S. Kim, I. S. Hwang, S. J. Kim, C. Y. Lee, and J. H. Lee, *Sens. Actuators, B Chem.* 135, 298 (**2008**).
14. L. Yang, R. M. Xing, Q. M. Shen, K. Jiang, F. Ye, J. Y. Wang, and Q. S. Ren, *J. Phys. Chem. B* 110, 10534 (**2006**).
15. W. B. Lu, X. Y. Qin, G. H. Chang, and X. P. Sun, *J. Nanosci. Nanotechnol.* 12, 2089 (**2012**).
16. S. H. Liu, B. S. Liu, K. Nakata, T. Ochiai, T. Murakami, and A. Fujishima, *J. Nanomater.* doi:10.1155/2012/491927 (**2012**).
17. J. Xu, C. G. Hu, H. Y. Han, M. Q. He, B. Wan, C. H. Xia, and Y. S. Tian, *J. Nanosci. Nanotechnol.* 11, 10829 (**2011**).
18. Z. L. Wang, *J. Nanosci. Nanotechnol.* 8, 27 (**2008**).
19. X. C. Wu, Y. R. Tao, L. Li, T. Y. Zhai, Y. Bando, and D. Golberg, *J. Nanosci. Nanotechnol.* 11, 10123 (**2011**).
20. H. Y. Li, M. Eastman, R. Schaller, W. Hudson, and J. Jiao, *J. Nanosci. Nanotechnol.* 11, 8517 (**2011**).
21. R. M. Xing and S. H. Liu, *Nanoscale* 4, 3135 (**2012**).
22. H. Zheng, G. Chen, F. Song, L. DeLouise, and Z. Y. Lou, *J. Biomed. Nanotechnol.* 7, 648 (**2011**).
23. R. M. Xing, J. H. Guo, C. L. Miao, S. H. Liu, and H. C. Pan, *J. Exp. Nanosci*. doi: 10.1080/17458080.2012.678891 (**2012**).
24. G. Misra, M. Goyal, S. Tenguria, and P. Tripathi, *J. Biomed. Nanotechnol.* 7, 191 (**2011**).

RESEARCH ARTICLE

**25.** G. H. Li, Y. Jiang, C. Wang, J. F. Shi, and Z. P. Zhang, *J. Nanosci. Nanotechnol.* 8, 3883 **(2008)**.
**26.** K. C. Kavya, R. Dixit, R. Jayakumar, S. V. Nair, and K. P. Chennazhi, *J. Biomed. Nanotechnol.* 8, 149 **(2012)**.
**27.** T. Schneider, A. Baldauf, L. A. Ba, V. Jamier, K. Khairan, M. Sarakbi, N. Reum, M. Schneider, A. Röseler, K. Becker, T. Burkholz, P. G. Winyard, M. Kelkel, M. Diederich, and C. Jacob, *J. Biomed. Nanotechnol*. 7, 395 **(2011)**.
**28.** W. D. Xiang, G. Y. Ji, J. Wei, Y. X. Yang, H. M. Yuan, and X. N. Liu, *J. Nanosci. Nanotechnol.* 11, 7820 **(2004)**.
**29.** D. S. Wang, C. H. Hao, W. Zheng, X. L. Ma, D. R. Chu, Q. Peng, and Y. D. Li, *Nano Research.* 2, 130 **(2009)**.
**30.** X. Wang, L. Li, S. T. Wang, Q. H. Guo, Z. D. Zhang, and Y. T. Qian, *J. Nanosci. Nanotechnol.* 6, 2042 **(2006)**.
**31.** J. H. Kim, H. Park, C. H. Hsu, and J. Xu, *J. Phys. Chem. C* 114, 9634 **(2010)**.
**32.** Y. J. Xiao, H. Q. Cao, K. Y. Liu, S. C. Zhang, and V. Chernow, *Nanotechnology* 21, 8 **(2010)**.
**33.** N. Petkov, J. Xu, M. A. Morris, and J. A. Holmes, *J. Phys. Chem. C* 112, 7345 **(2008)**.
**34.** Y. Q. He, J. P. Gao, Z. L. Li, J. Yang, Y. Liu, and X. D. Wang, *J. Nanosci. Nanotechnol.* 10, 532 **(2011)**.
**35.** Z. P. Liu, J. B. Liang, S. Li, S. Peng, and Y. Qian, *Chem.-Eur. J.* 10, 634 **(2004)**.
**36.** Z. P. Liu, S. Peng, Q. Xie, Z. K. Hu, Y. Yang, S. Y. Zhang, and Y. T. Qian, *Adv. Mater.* 15, 936 **(2003)**.
**37.** C. X. Song, D. B. Wang, T. Yang, and Z. S. Hu, *Cryst. Eng. Comm.* 13, 3087 **(2011)**.
**38.** W. X. Zhang, Z. H. Yang, X. M. Huang, S. Y. Zhang, W. C. Yu, Y. T. Qian, Y. B. Jia, G. Zhou, and L. Chen, *Solid State Commun.* 110, 143 **(2001)**.
**39.** S. H. Liu, S. F. Tian, and R. M. Xing, *Cryst. Eng. Comm.* 13, 7258 **(2011)**.
**40.** S. H. Liu, F. Lu, and J. J. Zhu, *Chem. Commun.* 47, 2661 **(2011)**.
**41.** S. H. Liu, F. Lu, X. D. Jia, F. F. Cheng, L. P. Jiang, and J. J. Zhu, *Cryst. Eng. Comm.* 13, 2425 **(2011)**.

Received: 3 December 2011. Accepted: 25 July 2012.